Nonlinear Reduced Order Model for Aeroelastic Static Deformations of Cantilevered Rectangular High Aspect Ratio Wing Model

T.Chandrasegaran, M.Y.Harmin, N.A.Rosly

Abstract*: The paper is motivated by the increasing interest in the use of high aspect ratio (HAR) wings to utilize its aerodynamic properties to gain better endurance. Nevertheless, the drawback of the issue is that with increment in the aspect ratio of the wing, the geometric nonlinearity gains more significance hence the linear solution is no longer acceptable. Even though, a number of nonlinear solution package are available in the market, but the solution is a very time consuming process. Hence, to help reduce the complexity of the nonlinear aeroelastic analysis, a Combined Model/Finite Element (CMFE) technique is employed to develop a Nonlinear Reduced Order Model (NROM) which describe the nonlinearity of the HAR wing from a solution of nonlinear static analysis for a range of prescribed loading cases. Three loading types were considered for the production of the NROM of which the force subjected to the wing model was normalized to follow the normal mode of the wing model. The three loading types are of the first bending mode, the first torsional mode and a combination of the first bending and torsional modes. The NROM equations are then developed utilizing the backward regression method. In order to verify the NROM equation accuracy with respect to the results obtained from the finite element analysis (FEA) software, the comparisons are made in terms of mean error and standard deviation of the error. The results indicate the NROM developed using a combination of the first bending mode and first torsional mode of the wing model has better accuracy than the NROM developed with the modes individually. The NROM also portrays greater accuracy when developed using the data due to the load from the first bending and the first torsional mode.

Keywords*: Combined Model/Finite Element (CMFE), high aspect ratio wing, nonlinear.

I. INTRODUCTION

The aviation industry has become one of the most sought after transportation service in recent years and this trend is most likely to skyrocket. By 2050, it is expected that air travel will be utilized by approximately 16 billion passengers [1]. Since, the aviation industry is to bloom, the pollution due to the aircrafts will increase with it as well. In order to curb this potential mishap, aircraft manufacturers are in favor of using technology to reduce the emission of the aircrafts. A potential technology to enable the reduction of the emission of the aircraft by utilizing the aerodynamic properties of the HAR wing. Generally, a high aspect ratio wing is said to be efficient as it will have a greater lift to drag ratio. A higher lift to drag ratio aircrafts are more efficient since the aircrafts are able to generate more lift with every increment of drag and also less induced drag will be generated due to the shape of the wings. It is also known that a whopping 43% of drag is constituent of induced drag. By reducing the induced drag, there will be a better lift to drag ratio which results in better efficiency. This will be beneficial as the aircrafts can travel longer. However, the problem with high aspect ratio wings are these wings are susceptible to geometric nonlinearity as these wings will have a larger wing deformation. High aspect ratio wings with long spans have a higher risk to face structural nonlinearity due to coupling of chord bending mode, torsion mode and flap bending mode. The continuous action of aerodynamic forces and resulting large deflection promotes geometrical nonlinearity on the HAR wing. Due to a limited understanding on the geometric nonlinearity of the HAR wing, the implementation of the HAR wing concept is limited. Moreover, the wings are prone to higher deflections at same conditions compared to the aircraft having a lower aspect ratio causing drastic changes in the wing's aeroelastic and dynamic behavior [2],[3],[4].

With the significance of geometric nonlinearity in mind, a number of techniques have been published and discuss on the geometrical nonlinearity analysis. Conventionally, the Nonlinear Finite Element Method (FEM) is employed, however the high computational time is a set-back. Therefore, the NROM can be employed to further reduce the complexity of the nonlinear solution resulting which offer into significant reduction in computational time [5],[6]. McEwan et al. suggested a combined modal/Finite Element (CMFE) technique to describe the nonlinearity of the HAR wing modal [7]. In the study, the displacement results were curve-fitted using regression analysis to describe the nonlinear stiffness term. The method was further extended by Harmin et al. by using the CMFE technique to model the geometric nonlinearity of a HAR wing model. The technique was used to conduct static deflection analysis, limit cycle oscillation and gust response analysis [4]. Thinesh et al. conducted a NROM analysis with the CMFE approach on a wing plate to describe the effect of mode selection and data selection on the accuracy of the NROM [6].

Revised Manuscript Received on October 15, 2019

***** Correspondence Author

Thinesh Chandrasegaran, Department of Aerospace, Faculty of Engineering, Universiti Putra Malaysia, Serdang, Malaysia Email: Thinesh7894@gmail.com

Dr.Mohammad Yazdi Harmin*, Department of Aerospace, Faculty of Engineering, Universiti Putra Malaysia, Serdang, Malaysia Email: myazdi@upm.edu.my

Nor Asyikin binti Rosly, Department of Aerospace, Faculty of Engineering, Universiti Putra Malaysia, Serdang, Malaysia Email: syikinrosly@gmail.com

II. METHODOLOGY

A. *Flowchart*

The study starts with aerostatic analysis of the HAR wing model. The analysis is conducted with the angle of attack and velocity being the manipulated variables. The corresponding load vector due to the selected angle of attack and velocity is extracted and is implied on the HAR wing model to be used in the linear and nonlinear static analysis. The linear analysis results is verified back with the aerostatic analysis since the aerostatic analysis conducted is in the linear condition. The verification of the results instills confidence in the use of the load vectors in the nonlinear analysis.

As for the NROM analysis, the test-cases to be used in the development of the NROM are defined to cover the bending and twist deflections of the HAR wing during the aerostatic analysis. Using the CMFE technique, the NROM polynomial can then be uncovered. In order to optimize the equation, a backward regression method is implied to get the most simplified equation without significant lost in accuracy.

The load vector used to simulate the linear and nonlinear analysis is used as input for the NROM to predict the corresponding deformation. The NROM deformation and nonlinear static analysis deformation are verified to investigate the NROM accuracy by computing the mean error and its corresponding standard deviation. Fig. 1 summarizes the overall procedure that involved in this work.

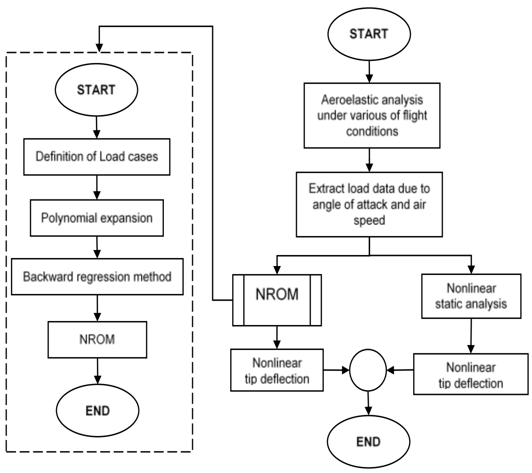

Fig. 1 Flowchart of the study

B. *HAR Wing Model*

The HAR wing simulation model consists of 16 sections based on Rosly N.A [8] as illustrated in Fig. 2. 17 ribs were equally spaced along the leading and trailing edge spars on the HAR wing model. The material and geometric properties of the beam are summarized in Table 1.

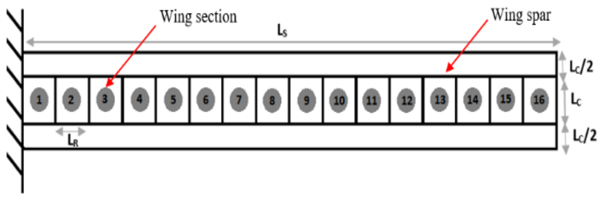

(L_S = span length, L_C = plate chord length, L_R = rib length)
Fig. 2 Layout of HAR wing model

TABLE 1
DESIGN PARAMETERS OF THE HAR WING MODEL

Material and geometric properties of	HAR wing
Span length, L_S	0.8 m
Plate chord length, L_C	0.025 m
Density of spring steel-plate, ρ_{ss}	7833.413 kgm^{-3}
Poisson's ratio of spring steel-plate, υ_{ss}	0.295

C. *Normal Mode Analysis*

The HAR wing model described above is simulate through a normal mode analysis in order to obtain the normal mode properties which are the eigenvalue and its corresponding eigenvectors. The normal modes considered for the NROM development and for the load case are the first bending mode and first torsional mode which corresponds to the first mode and sixth mode respectively. Table 2 details the modes that being considered in this work.

TABLE 2
MODES IN THE ESTABLISHMENT OF NROM

Mode	Type of modes	Eigenvalues
1	1st bending	90.4111
6	1st torsion	256100.6

D. *Aerostatic Analysis*

Aerostatic analysis was conducted on the HAR wing model with varying velocity and angle of attack to study its load force. The analysis was conducted for a velocity of 5 ms^{-1} to 40 ms^{-1} with a range of angle of attack from 1^{o} to 5^{o}. The procedure was conducted using MSC NASTRAN (SOL 144). The deflection of the wing model and its respective load force was extracted for respective angle of attacks and velocities.

E. *Finite Element Method*

Two stages are involved for this procedure. The first stage is to extract the load forces from the aerostatic analysis and run the linear and nonlinear static finite element analysis in MSC NASTRAN solution sequence of SOL 101 and SOL 106 respectively. The deflection is then curve-fitted to analyze the nonlinearity of the HAR wing model. A limitation is set to a maximum tip deflection of 0.4 m which is half of the wingspan. The angle of attack and velocity combination which causes the tip deflection of the HAR wing model to exceed 0.4 m is neglected. The second stage is to run the linear and nonlinear static finite element analysis for the production of the NROM. Three type of load cases have been described to analyze the effectiveness of the NROM.

The first load case type describes a force which acts on the HAR wing model is normalized to simulate the first bending mode. The analysis is conducted till the force selected has good coverage of linear and nonlinear properties. Fig. 3 shows the distribution of the first bending normalized force acting on the HAR wing model. Note that, the force is applied only on the plate. Whereas, Fig. 4 shows the tip deflection of HAR wing model due to the first bending normalized force acting on the HAR wing model for a range of defined force magnitude. From the figure, it can be seen that the tip deflection of the first load case type is able to cover the linear and nonlinear region hence is suitable to be used to characterize the NROM.

Retrieval Number: A9430109119/2019©BEIESP
DOI: 10.35940/ijeat.A9430.109119

Published By:
Blue Eyes Intelligence Engineering
& Sciences Publication

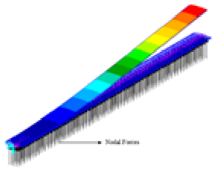

Fig. 3 Distribution of the first bending normalized force acting on the HAR wing model.

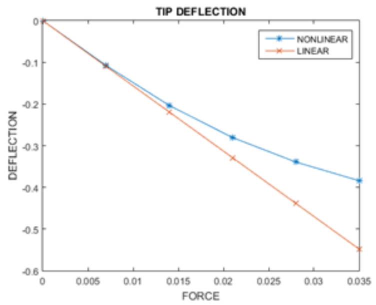

Fig. 4 Tip deflection due to normalized force with respect to first bending mode

The second type of load case described is to simulate a torsional effect on the HAR wing model. A force distribution is characterized with respect to the first torsional mode. The tip rotation of the forces are plotted to analyze the nonlinearity of the HAR wing model. Fig. 5 shows the distribution of the first torsional normalized force acting on the HAR wing model. Whereas Fig. 6 shows the tip rotation of the HAR wing model due to the first torsional normalized force in a range of defined force magnitude.

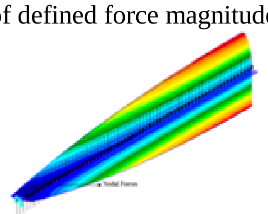

Fig. 5 Distribution of the first torsional normalized force acting on the HAR wing model

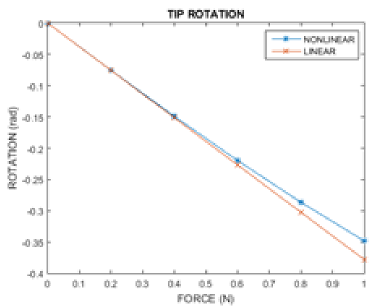

Fig. 6 Tip rotation for normalized force with respect to first torsional mode

The third type of load case described is to simulate a combination of bending and torsional effect on the HAR wing model. A force distribution is normalized with respect to the combination of first bending and first torsional modes to characterize a combination of bending and twist deflection on the wing model. The tip deflection and tip rotation of the forces are plotted to analyze the degree of nonlinearity that involved in this case. Fig. 7 shows the distribution of the combination of first bending and first torsional normalized force acting on the HAR wing model. Whereas Fig. 8 and Fig. 9 show the results of tip deflection and the tip rotation respectively for a range of defined force magnitude.

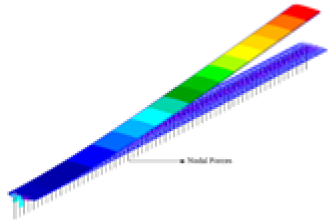

Fig. 7 Distribution of the first bending and first torsional normalized force acting on the leading edge of the HAR wing model

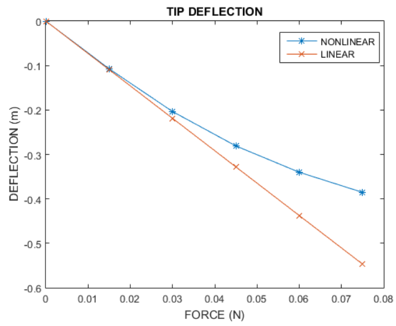

Fig. 8 Tip deflection for normalized force with respect to first bending and first torsional mode

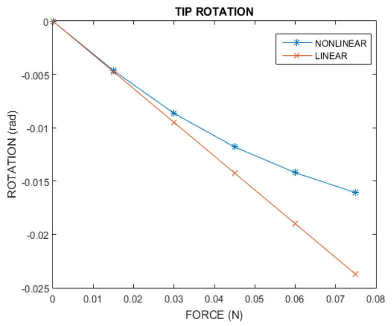

Fig. 9 Tip rotation for normalized force with respect to first bending and first torsional mode

F. *Nonlinear Reduced Order Model (NROM)*

NROM are developed using the aforementioned load cases via the CMFE technique and a backward regression analysis. After conducting the normal mode analysis and the verification of the nonlinearity of the HAR wing plate model, the force-displacement relationship is utilized to determine the nonlinear stiffness terms through curve fitting. The NROM equation undergoes a backward elimination process to optimize the equation without compromising on its accuracy. With the NROM equation characterized with the nonlinear stiffness term, the force input in modal space can be inserted to obtain the corresponding modal displacement value. The modal displacement value then can be converted into physical displacement by utilizing the eigenvector of the mode used to characterize the equation. The output is then verified with the FEA data to calculate its accuracy in terms of mean error and standard deviation of the error.

The mathematical modelling used by Harmin et al. [4] for the static system equation, where $[\boldsymbol{E_L}]$ is assembled linear stiffness matrices of size NR × NR; $\{\boldsymbol{F}\}$ is the NR × 1 applied modal force; $\{\boldsymbol{E_{NL}}(p)\}$ is a polynomial form as the product of Nth order modal displacements multiplied by the yet to be defined nonlinear stiffness coefficients and p is the modal displacement.

$$[\boldsymbol{E_L}]\{p\} + \{\boldsymbol{E_{NL}}(p)\} = \{\boldsymbol{F}\} \qquad (2)$$

The left-hand side of the equation consists of the restoring stiffness force for both linear stiffness as well as nonlinear stiffness. By rearranging equation (2):

$$\{\boldsymbol{F}\} - [\boldsymbol{E_L}]\{p\} = \{\boldsymbol{E_{NL}}(p)\} \qquad (3)$$

From the equation above, let:

$$[D] = [\{\boldsymbol{F}\} - [\boldsymbol{E_L}]\{p\}] \qquad (4)$$

where D is 1 × NL vector; NL is the number of load cases considered for the investigation. Since $\{\boldsymbol{E_{NL}}(p)\}$ is a polynomial function hence the matrix is split into:

$$\{\boldsymbol{E_{NL}}(p)\} = [p^2 \quad p^3 \quad \cdots] \begin{bmatrix} A_1 \\ A_2 \\ \vdots \end{bmatrix} \qquad (5)$$

where A_1 and A_2 are the constants in the polynomial equation. The polynomial constants can be determined by:

$$\begin{bmatrix} A_1 \\ A_2 \\ \vdots \end{bmatrix} = [D]\,[p^2\ p^3 \ldots]^{inv} \qquad (6)$$

where $[p^2 \ \ p^3 \cdots]^{inv}$ is the pseudo-inverse of the $[p^2 \ \ p^3 \ \cdots]$ matrix. Once the coefficients of the polynomial are determined, the NROM equations can then be formed. In order to optimize the equation, a backward elimination procedure is carried out.

The NROM polynomial expression was evaluated up to the third order of the defined mode, r;

$$\boldsymbol{E}_{NL_{(r)}}\left(p_1, p_2, p_{NR}\right) =$$

$$\sum_{s=1}^{NR}\sum_{i=2}^{3} A_r p_s^i + \sum_{s=1}^{NR-1}\sum_{s+1}^{NR}\sum_{i=1}^{2}\sum_{j=1}^{3-i} A_r = p_s^i p_t^j \quad (7)$$

The nonlinear restoring force is fitted to determine the unknown nonlinear modal stiffness coefficients. The nonlinear restoring force a mode of r can be illustrated as;

$$\begin{Bmatrix} f_{r_{(1)}} - \boldsymbol{E}_{L_{(r)}} p_{r_{(1)}} \\ f_{r_{(2)}} - \boldsymbol{E}_{L_{(r)}} p_{r_{(2)}} \\ \vdots \\ \vdots \\ f_{r_{(NT)}} - \boldsymbol{E}_{L_{(r)}} p_{r_{(NT)}} \end{Bmatrix} =$$

$$\begin{bmatrix} p_{1\,(1)}^2 & p_{1(1)}^3 & \cdots & \cdots \\ p_{1\,(2)}^2 & p_{1(2)}^3 & \cdots & \cdots \\ \vdots & \vdots & \cdots & \cdots \\ \vdots & \vdots & \cdots & \cdots \\ p_{1\,(NT)}^2 & p_{1(NT)}^3 & \cdots & \cdots \end{bmatrix} \begin{Bmatrix} A_{r_{(1)}} \\ A_{r_{(2)}} \\ \vdots \\ \vdots \\ A_{r_{(NA)}} \end{Bmatrix} \quad (8)$$

Equation (8) can be also represented as;

$$\{f_r\}_{NL} \approx \{\tilde{f}_r\}_{NL} = [\boldsymbol{D}_r]\{A_r\} \qquad (9)$$

where $\{\tilde{f}_r\}_{NL}$ is the NT × 1 vector of fitted values of nonlinear modal stiffness restoring forces, $[\boldsymbol{D}_r]$ is NT × NA design matrix and $\{A_r\}$ is NA × 1 vector containing the yet to be defined nonlinear stiffness figure. The nonlinear stiffness coefficient $\{A_r\}$ was evaluated using the singular value decomposition (SVD) technique. After such, the backward elimination method was utilized to remove the less significant nonlinear polynomial terms which don't impact the accuracy the overall solution with great significance.

In order to calculate the modal displacement for a defined force, the Newton Raphson method analysis is deployed on the NROM equation. The modal force can be obtained by referring to (10) where the ψ is the N × NR matrix of the linear mode shapes of the selected mode while the physical displacement, x can be obtained by referring to (11).

$$\{\boldsymbol{F}\} = [\psi]\,\{\mathbb{F}\} \qquad (10)$$

$$[x] = [\psi]^{\nu}\,[p] \qquad (11)$$

The accuracy of the NROM is verified with the conventional FEA analysis. The accuracy is evaluated by calculating the mean and standard deviation of the error for each case and is displayed graphically. The aforementioned error is the differences between the solution obtained by NROM and FEA of the nonlinear static solution.

III. RESULTS AND DISCUSSION

A. *Prediction of nonlinear aerostatic deflection using combination of load case type 1 and load case type 2 (CASE 1).*

The NROM is described using the data collected from the first bending and first torsional mode normalized force, characterized by the first torsional and bending mode. Figure 10 and Figure 11 shows the mean error and standard deviation of the error for bending and twist deflection of NROM-CASE 1 for different angle of attacks respectively. Table 3 and Table 4 displays the maximum mean error of NROM-CASE 1 for bending and twist deflection respectively. From the results, it can be noted that the maximum mean error increases as the deflection is higher in magnitude which results from the increment of airspeed as well as angle of attack. Nevertheless, the maximum mean error indicates the value is insignificant in comparison to the deflection of the wing for both bending and twist.

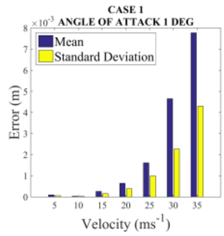

(a) AOA = 1

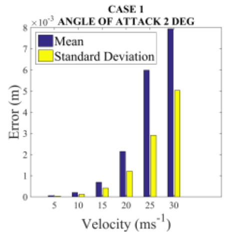

(b) AOA = 2

Retrieval Number: A9430109119/2019©BEIESP
DOI: 10.35940/ijeat.A9430.109119

Published By:
Blue Eyes Intelligence Engineering
& Sciences Publication

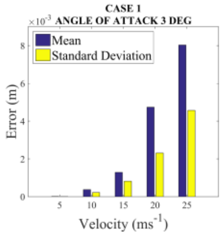

(c) AOA = 3

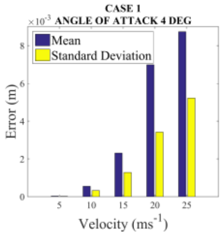

(d) AOA = 4

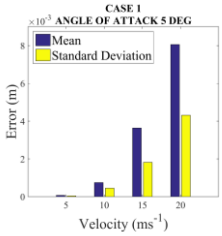

(e) AOA = 5

Fig 10. Mean error and standard deviation of NROM-CASE 1 prediction of bending deflection of wing

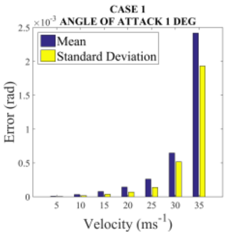

(a) AOA = 1

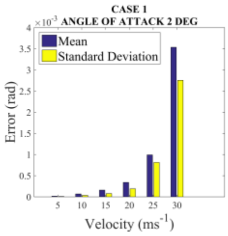

(b) AOA = 2

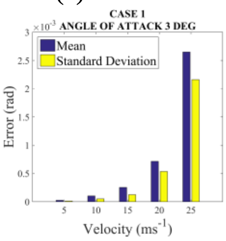

(c) AOA = 3

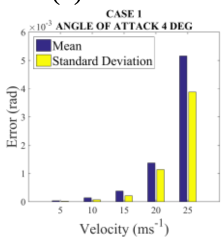

(d) AOA = 4

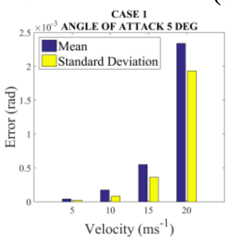

(e) AOA = 5

Fig 11. Mean error and standard deviation of NROM-CASE 1 prediction of twist deflection of wing

Table 3
Maximum Mean Error For Bending Deflection (Mm)

AOA	Velocity (ms^{-1})							
	5	10	15	20	25	30	35	40
1^o	0.1	0	0.3	0.6	1.6	4.7	7.8	
2^o	0.1	0.2	0.7	2.1	6.0	7.9		
3^o	0	0.4	1.3	4.7	8.0			
4^o	0	0.5	2.3	7.0	8.7			
5^o	0.1	0.7	3.6	8.1				

*Note: The shaded section has nonlinear deflections above the constraints hence the results weren't included in the study.

Table 4
Maximum Mean Error For Twist Deflection (Rad)

AOA	Velocity (ms^{-1})							
	5	10	15	20	25	30	35	40
1^o	0	0	0.1	0.1	0.3	0.6	2.4	
2^o	0	0.1	0.2	0.3	1.0	3.5		
3^o	0	0.1	0.3	0.7	2.6			
4^o	0	0.1	0.4	1.4	5.2			
5^o	0	0.2	0.6	2.3				

*Note: The shaded section has nonlinear deflections above the constraints hence the results weren't included in the study.

B. *Prediction of nonlinear aerostatic deflection using NROM from load case type 3 (CASE 2).*

The NROM is described using the data collected from the first bending and first torsional mode normalized force, characterized by the first torsional and bending mode. Figure 12 and 13 shows the mean error and standard deviation of the error of bending and twist deflection for NROM-CASE 2 for different angle of attacks. Table 5 and Table 6 displays the maximum mean error of NROM-CASE 1 for bending and twist deflection respectively. From the obtained results, the NROM-CASE 2 was able to predict the deflection of the wing with significant accuracy. The maximum mean error increases with higher deflection in magnitude of the wing model. The maximum mean error for NROM-CASE 2 also shows good accuracy. Although, both NROMs have similar maximum mean error for bending deflection, the NROM-CASE 1 has a better accuracy in predicting the twist deflection of the wing model.

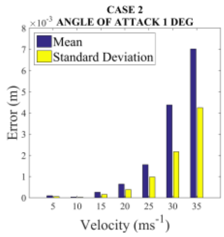

(a) AOA = 1

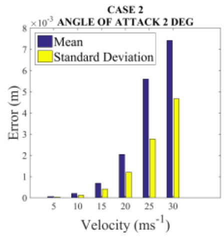

(b) AOA = 2

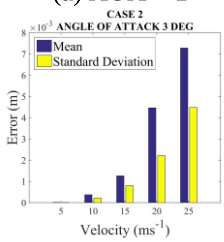

(c) AOA = 3

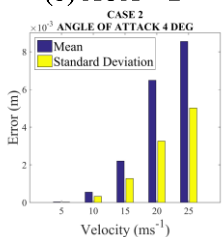

(d) AOA = 4

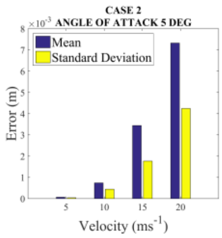

(e) AOA = 5

Fig 12. Mean error and standard deviation of NROM-CASE 2 prediction of bending deflection of wing

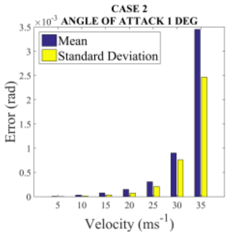

(a) AOA = 1

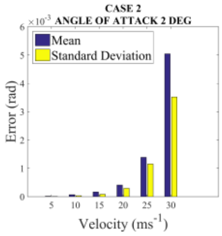

(b) AOA = 2

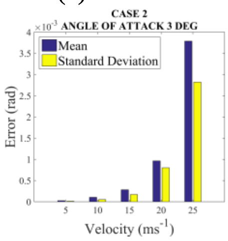

(c) AOA = 3

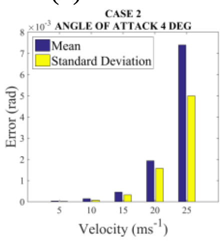

(d) AOA = 4

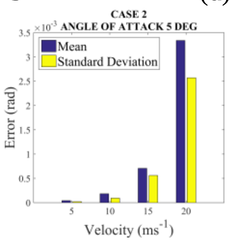

(e) AOA = 5

Fig 13. Mean error and standard deviation of NROM-CASE 2 prediction of twist deflection of wing

TABLE 5
MAXIMUM MEAN ERROR FOR BENDING DEFLECTION (mm)

AOA	Velocity (ms^{-1})							
	5	10	15	20	25	30	35	40
1^o	0.1	0	0.3	0.6	1.6	4.4	7.0	
2^o	0.1	0.2	0.7	2.0	5.6	7.4		
3^o	0	0.5	2.2	6.5	8.5			
4^o	0	0.5	2.3	7.0	8.7			
5^o	0.1	0.7	3.4	7.3				

*Note: The shaded section has nonlinear deflections above the constraints hence the results weren't included in the study.

Table 6
Maximum Mean Error For Twist Deflection (Rad)

AOA	Velocity (ms^{-1})							
	5	10	15	20	25	30	35	40
1^o	0	0	0.1	0.2	0.3	0.9	3.5	
2^o	0	0.1	0.2	0.4	1.4	5.0		
3^o	0	0.1	0.3	1.0	3.8			
4^o	0	0.1	0.5	1.9	7.4			
5^o	0	0.2	0.7	3.3				

*Note: The shaded section has nonlinear deflections above the constraints hence the results weren't included in the study.

IV. CONCLUSIONS

The NROM produced from the two types of cases described to characterize the nonlinearity of the HAR wing model has been demonstrated. The three load types described to capture the bending deflection based on first bending mode profile, twist deflection based on the first torsional mode and a combination of both bending and twist deflection to produce NROMs can be summarized to sufficiently significant. The NROM based on case 1 where load case 1 and load case 2 were implemented was able to predict the nonlinear static deformation with more accuracy in comparison to the NROM based on case 2. The NROM based on case 1 has been developed with higher twist deflection properties in comparison to the other NROM hence explaining the higher accuracy when predicting the nonlinear twist deflection. It is also noted that the accuracy of the NROM is subjected to the maximum deflection of the wing model in the load case defined. The NROM fails to predict any deformation exceeding the maximum input deflection during the production of the NROM. Table 7 summarize the maximum mean error of each NROM.

TABLE 7
MAXIMUM MEAN ERROR OF NROM

NROM	Bending deflection (m)	Twist deflection (rad)
1	0.0087	0.052
2	0.0087	0.074

ACKNOWLEDGMENT

The authors acknowledge the financial support from Ministry of Education (MOE) Malaysia for this study through the Fundamental Research Grant Scheme (FRGS/1/2015/TK09/UPM/02/2) with Project Code: 03-01-15-1625FR.

REFERENCES

1. Iata.org. (2011). [online] Available at: https://www.iata.org/pressroom/facts_figures/documents/vision-2050.pdf [Accessed 20 Aug. 2019].
2. F. Afonso, L. Goncalo, J. Vale, E. L. Oliveira, F. Lau & A. Suleman, Linear vs non-linear aeroelastic analysis of high apect-ratio wings. Congr. Metod. Numer. em Eng., pp. 1–9, 2015.
3. M. Smith, M. Patil & D. Hodges, CFD-based analysis of nonlinear aeroelastic behavior of high-aspect ratio wings. 19th AIAA Applied Aerodynamics Conference, Fluid Dynamics, pp. 1-10, 2001.
4. M. Y. Harmin and J. E. Cooper, Aeroelastic behaviour of a wing including geometric nonlinearities. Aeronaut. J., vol. 115, no. 1174, pp. 767–777, 2011.
5. S. Chae, Effect of follower forces on aeroelastic stability of flexible structure (Doctoral dissertation), 2004. Retrieved from: https://smartech.gatech.edu/bitstream/handle/1853/5037/chae_seungmseu_200407_phd.pdf
6. Thinesh.C & M.Y. Harmin, Nonlinear reduced order model of high aspect ratio rectangular wing plates. International Journal of Engineering & Technology Vol. 7, 2018
7. McEwan MI, Wright JR, Cooper JE, Leung AYT, A combined modal/finite element analysis technique for the dynamic response of a nonlinear beam to harmonic excitation. Journal of Sound and Vibration;243(4): 601-24, 2001.
8. Rosly, N. A., & Harmin, M. Y., Finite element analysis of high aspect ratio wind tunnel wing model: A parametric study. IOP Conference Series: Materials Science and Engineering,270, 2017.
9. MSC Software (2013). Bulk Data Entry Descriptions. In MSC Nastran Quick Reference Guide (pp. 2007). Retrieved from: https://simcompanion.mscsoftware.com/resources/sites/MSC/content/meta/DOCUMENTATION/10000/DOC10525/~secure/n

astran_2013.1.1_quick_reference_guide.pdf

AUTHORS PROFILE

Thinesh Chandrasegaran is currently a student pursuing his MSc in Universiti Putra Malaysia (UPM). He graduated from UPM with Bachelor of Engineering Aerospace degree with first class honors. For his bachelor final year project, he was awarded a gold medal for his poster presentation on his study on the Nonlinear Order Reduced Aeroelastic Model which was accessed by the industrial counter-parts. The award was a stepping stone for him to be awarded the 'Best Final Year Project' in the year 2018. Through his experience in 2 years research study, he is able to publish one journal paper and one submitted.

Dr. Mohammad Yazdi Harmin started his career at Universiti Putra Malaysia (UPM) as a Tutor upon completion of his Bachelor of Aerospace Engineering (UPM) back in 2002. After five years of serving, he has pursued his PhD in Aeroelastic Modelling & Design at the University of Liverpool. He rejoined UPM and served as a Senior Lecturer upon completion of his PhD in 2012. He is a registered member of Board of Engineers Malaysia since 2013 and a founding member of Aerospace Malaysia Society. Dr. Mohammad Yazdi's main research interests lie in the fields of aerolastic modelling, design and testing. He has published over 20 journal publications and conference articles in the aforementioned topics and has received several grants from various funding agencies. He is currently the leader for two UPM grants and one Ministry of Higher Education grant and the co-investigator for eight other grants. In term of teaching, he has taught a wide range of aerospace related courses at the undergraduate and graduate levels, including aeroelasticity, flight mechanics, structural dynamics, aircraft design, engineering optimisation and computer programming. As a main supervisor, he has successfully produced and supervising a number of postgraduate holders and students (Master & PhD) in various aerospace engineering sub-expertises.

Nur Asyikin Rosly is currently a student pursuing her MSc in Universiti Putra Malaysia (UPM). During her Bachelor of Aerospace Engineering at UPM, she was awarded with scholarship from JPA. The first two years of her master study, she was assigned as an instructor for undergraduate student at aerodynamic lab. Her master research focuses on the study of high aspect ratio wing model subjected to a geometric nonlinearity, which consisted of two main parts; the simulation and experimental parts. She has a first-hand experience in conducting a ground vibration testing using impact hammer test, and wind tunnel flutter testing. As of today, she has published one journal publication and one conference article.